

5–10 GeV Neutrinos from Gamma-Ray Burst Fireballs

John N. Bahcall¹ and Peter Mészáros^{1,2}

¹*Institute for Advanced Study, School of Natural Sciences, Einstein Drive, Princeton, New Jersey 08540*

²*Pennsylvania State University, 525 Davey Lab, University Park, Pennsylvania 16802*

(Received 3 April 2000)

A gamma-ray burst fireball is likely to contain an admixture of neutrons. Inelastic collisions between differentially streaming protons and neutrons in the fireball produce ν_μ ($\bar{\nu}_\mu$) of ~ 10 GeV as well as ν_e ($\bar{\nu}_e$) of ~ 5 GeV, which could produce ~ 7 events/year in km^3 detectors, if the neutron abundance is comparable to that of protons. Photons of ~ 10 GeV from π^0 decay and ~ 100 MeV $\bar{\nu}_e$ from neutron decay are also produced, but will be difficult to detect. Photons with energies ≤ 1 MeV from shocks following neutron decay produce a characteristic signal which may be distinguishable from the proton-related MeV photons.

PACS numbers: 96.40.Tv, 98.70.Rz, 98.70.Sa

I. Introduction.—Gamma-ray burst (GRB) sources are distributed throughout the universe and their energy output is measured to be a substantial fraction of a solar rest mass equivalent [1]. A variety of observations support the interpretation that these events are caused by cataclysmic stellar collapse or compact mergers, producing a fireball with bulk expansion Lorentz factor $\Gamma \sim 10^2$ – 10^3 . In the standard GRB model a fireball made up of γ , e^\pm , and magnetic fields with an admixture of baryons is produced by the release of a large amount of energy $E \geq 10^{53}$ ergs in a region $r_o \sim 10^7 r_{o7}$ cm (e.g., [2]). The observations indicate that typical fireballs are characterized by a luminosity $L \sim 10^{52} L_{52}$ erg s⁻¹ and durations $t_w = 10 t_{w1}$ s in the observer frame, with a large spread in both quantities. The outflow is controlled by the value of the dimensionless entropy $\eta = (L/\dot{M}c^2)$ injected at r_o . Previous discussions of fireball models have generally focused on the charged particle components, since they determine directly the photon signal. However, consideration of a neutron component introduces qualitatively new effects [3]. In a p, n fireball, for values of $\eta \geq 400$, the neutrons and protons acquire a relative drift velocity causing inelastic n, p collisions and creating neutrinos.

We investigate here the neutrino and photon signals from n, p collisions following decoupling in GRB. The ~ 10 GeV neutrinos from this mechanism depend upon the presence of neutrons in the original explosion, but the neutrinos are created in simple physical processes occurring in the later stages of the fireball. On the other hand, the 10^5 GeV neutrinos discussed in Ref. [4] require the acceleration in shock waves of ultrahigh energy protons interacting with photons. Thus the 10 and 10^5 GeV neutrinos reflect very different astrophysical processes and uncertainties. Other processes, e.g., neutrinos from p, p collisions [5] also require shocks but have lower efficiencies, while 10 – 30 MeV neutrinos from the original explosion [6] are much harder to detect due to the lower cross sections.

We show (Sec. III) that the 10 GeV neutrinos could be detectable by future km^3 size detectors. The associated

~ 10 GeV γ -ray fluences are compatible with current detection rates, and may be detectable with future space missions. The dependence of these signals on the neutron/proton ratio ξ provides a new tool to investigate the nature of the GRB progenitor systems. Moreover, the predicted neutrino event rate depends on the asymptotic bulk Lorentz factor of the neutrons, which is linked to that of the protons. The latter affects all of the electromagnetic observables from the GRB fireball, including the photospheric and shock radii, as well as the particle acceleration and nonthermal photon production.

II. Dynamics, n - p decoupling and pions.—Above the fireball injection radius r_o , the outflow velocity increases through conversion of internal energy into kinetic energy, the bulk Lorentz factor Γ varying as $\Gamma \sim T'_o/T' = r/r_o$, where T' is the comoving temperature and $T'_o = 1.2 L_{52}^{1/4} r_{o7}^{-1/2}$ MeV is the initial temperature at r_o (henceforth denoting with primes the quantities measured in the comoving frame). The flow may be considered spherical, which is also a valid approximation for a collimated outflow of opening angle $\theta_j > \Gamma^{-1}$, for the conditions discussed here. In a pure proton outflow the linear growth of Γ saturates when it reaches an asymptotic value $\Gamma_f \leq \eta \sim \text{const}$, the value η being achieved when the fireball converts all of its luminosity into expansion kinetic energy. For an n, p fireball, beyond the injection radius r_o the comoving temperature is low and nuclear reactions are rare, so the n/p ratio ξ remains constant. Since the thermal velocities are nonrelativistic, decoupling of the n and p fluids is essential for high-energy neutrino production.

At the base of the outflow the n and p components are coupled by nuclear elastic scattering. In terms of the center-of-mass (c.m.) relative energy ϵ_{rel} and the relative velocity v_{rel} between nucleons, $\sigma'_{\text{el}} v'_{\text{rel}} \sim \sigma_o c$. The c.m. energy dependence $\sigma_{\text{el}} \propto \epsilon'^{-1/2} \propto v'^{-1}_{\text{rel}}$ is approximately valid between energies ~ 1 MeV and the pion production threshold ~ 140 MeV, and $\sigma_o \sim \sigma_\pi \sim 3 \times 10^{-26}$ cm² is the pion formation cross section above threshold. The p and n are cold in the comoving frame,

and remain well coupled until the comoving n, p scattering time $t'_{np} \sim (n'_p \sigma_o c)^{-1}$ becomes longer than the comoving expansion time $t'_{exp} \sim r/c\Gamma$. Denoting the comoving neutron density $n'_n = \xi n'_p$ with $\xi \lesssim 1$, mass conservation implies $n'_p = L/[(1 + \xi)4\pi r^2 m_p c^3 \Gamma \eta]$. The n, p decoupling occurs in the coasting or accelerating regimes depending on whether the dimensionless entropy η is below or above the critical value

$$\begin{aligned} \eta_\pi &= [L\sigma_\pi/4\pi m_p c^3 r_o(1 + \xi)]^{1/4} \\ &\simeq 3.9 \times 10^2 L_{52}^{1/4} r_o^{-1/4} ([1 + \xi]/2)^{-1/4}. \end{aligned} \quad (1)$$

Figure 1 shows the dependence of Γ on radius for different η . For low values, $\eta \lesssim \eta_\pi$, the condition $t'_{np} \gtrsim t'_{exp}$ is achieved at a radius $r_{np}/r_o = \eta_\pi(\eta_\pi/\eta)^3$, which is beyond the saturation radius $r_s/r_o \sim \eta$ at which both n and p start to coast with $\Gamma \sim \eta = \text{const}$. In this case, even after decoupling both n and p continue to coast together due to inertia, and their relative velocities never reach the threshold for inelastic collisions.

For $\eta \gtrsim \eta_\pi$, on the other hand, the n, p decoupling condition $t'_{np} \gtrsim t'_{exp}$ occurs while the protons (and neutrons) are still accelerating as $\Gamma_p \simeq (r/r_o)$, at a radius

$$(r_{np}/r_o) = \eta_\pi(\eta/\eta_\pi)^{-1/3}, \quad \text{for } \eta \gtrsim \eta_\pi. \quad (2)$$

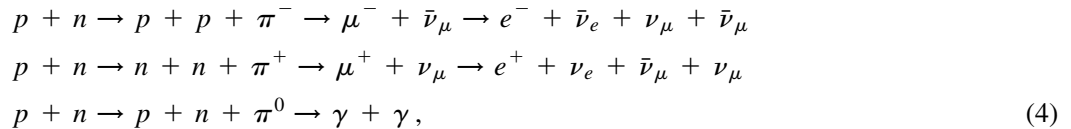
Beyond this decoupling radius, the p can still continue to accelerate with $\Gamma_p \propto r$ (as long as they remain coupled to the photons). However, the neutrons are no longer accelerated, since they only interact with the protons, and they continue to coast with the value of $\Gamma \sim \Gamma_{nf} \simeq \text{const}$ achieved up to that point,

$$\begin{aligned} \Gamma_{nf} &= (3/4)\eta_\pi(\eta/\eta_\pi)^{-1/3} \quad (\text{for } \eta \gtrsim \eta_\pi) \\ &\simeq 3 \times 10^2 L_{52}^{1/4} r_o^{-1/4} ([1 + \xi]/2)^{-1/4} (\eta/\eta_\pi)^{-1/3}, \end{aligned} \quad (3)$$

where the (3/4) factor comes from a numerical solution [3] of the coupling equations.

When the n, p decoupling condition $\eta \gtrsim \eta_\pi$ is satisfied, the relative n, p drift velocity $v_{rel} \rightarrow c$ and the inelastic pion production threshold $\epsilon' > 140$ MeV is reached. Since $\sigma_o \sim \sigma_\pi$, the condition $t'_{np} \sim t'_{exp}$ implies that the optical depth to pion formation is of order unity. Thus, for $\eta \gtrsim \eta_\pi$ the radius $r_{np} \equiv r_\pi$ is not only a decoupling radius but also an effective ‘‘pionospheric’’ radius.

The lowest energy threshold processes at r_π are



which occur in approximately equal ratios and with near unit total probability. The corresponding $p + p(n + n) \rightarrow \pi^\pm, \pi^0$ processes do not involve a relative drift velocity (as do the $p + n$), and are thus less probable. Processes leading to multiple baryons are also

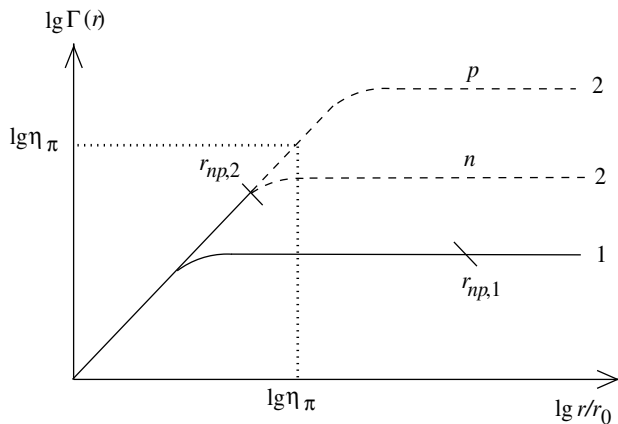


FIG. 1. Schematic behavior of the bulk Lorentz factor Γ as a function of radius r for various values of the dimensionless entropy η , the decoupling radius r_{np} being indicated with a diagonal slash. Curve 1 is for $\eta < \eta_\pi$, where the n and p achieve the same asymptotic $\Gamma_{nf} \sim \Gamma_{pf} \sim \eta$. Curve 2 is for $\eta > \eta_\pi$, and in this case n, p decoupling occurs before protons have reached their asymptotic Lorentz factor, which is larger than that of neutrons. This leads to inelastic n, p collisions, pion formation, and neutrino emission at $r_{np,2}$.

suppressed due to the higher threshold, and for simplicity we restrict ourselves to the above $p + n$ processes.

III. 10 GeV neutrinos and γ rays.—The total number of neutrons carried by the fireball is

$$\begin{aligned} N_n &= \left(\frac{\xi}{1 + \xi} \right) \frac{E}{\eta m_p c^2} \\ &\sim 0.83 \times 10^{53} E_{53} \left(\frac{2\xi}{1 + \xi} \right) \left(\frac{400}{\eta} \right), \end{aligned} \quad (5)$$

The comoving optical depth $\tau' \sim n'_p \sigma r / \Gamma \propto \sigma / (r\Gamma)$ has the same dependence for pion formation and photon scattering, but $\sigma_\pi \ll \sigma_T$ (Thomson cross section), so the pionosphere r_π occurs below the γ -photosphere r_γ . The γ rays in Eq. (4) can escape only from a skin depth below the γ sphere in the essentially laminar flow with probability $P_\gamma \lesssim \tau_\pi(r_\gamma) \sim r_\pi/r_\gamma \sim (\sigma_\pi/\sigma_T)(1 + \xi/7)^2 \sim 1/25$, for $\eta \gtrsim \eta_\pi$. Each n leads to ~ 1 photon of c.m. energy, $\epsilon'_\gamma \sim 70$ MeV, and observer energy centered broadly around $\epsilon_\gamma \sim 70\Gamma_{nf}/(1 + z)$ MeV ~ 10 GeV. By using a proper distance $D_p = 2.8 \times 10^{28} h_{65}^{-1} [1 - 1/\sqrt{1 + z}]$ cm with a Hubble constant $h_{65} = H_o/65$ km s $^{-1}$ Mpc $^{-1}$, the number fluence at Earth is $N_\gamma \sim N_n P_\gamma / 4\pi D_p^2 \sim 10^{-5}$ cm $^{-2}$. This is below the sensitivity of the ~ 200 cm 2 area EGRET detector at the Compton Gamma Ray Observatory (e.g., [7]), but for rare nearby bursts it may be detectable by GLAST [8].

The neutrinos originate at the pionospheric radius $r_\pi \ll r_\gamma$, where $\tau_\pi \sim 1$. In this region the stable charged products and γ rays from the reactions (4) remain in the fireball, and each n leads on average to one ν and one $\bar{\nu}$. We list below the average neutrino energies for pions and muons decaying at rest. The neutrinos from muon decay have a continuum spectrum. Also, the energies are Doppler broadened by $v_{rel}/c \sim 0.5$,

$$\begin{aligned} \epsilon'_{\bar{\nu}_\mu} &\approx 30 \text{ MeV}, & \epsilon'_{\nu_\mu} &\approx 30 \text{ MeV} & \text{from } \pi^\pm, \\ \epsilon'_{\nu_e} &\approx 30 \text{ MeV}, & \epsilon'_{\bar{\nu}_\mu} &\approx 50 \text{ MeV} & \text{from } \mu^+, \\ \epsilon'_{\bar{\nu}_e} &\approx 30 \text{ MeV}, & \epsilon'_{\nu_\mu} &\approx 50 \text{ MeV} & \text{from } \mu^-. \end{aligned} \quad (6)$$

The relevant cross section for detection averaged over ν and $\bar{\nu}$ is $\sigma_\nu \sim 0.5 \times 10^{-38} (\epsilon/\text{GeV}) \text{ cm}^2$ at the observed energy ϵ [9]. The observer frame energy is $\epsilon = \epsilon' \alpha \Gamma_{nf} / (1+z)$, where $\alpha \sim 1$ near threshold. For the c.m. $\nu\bar{\nu}$ production energies of Eq. (6), the average $\nu + \bar{\nu}$ c.m. energy per neutron is $\epsilon' \approx 100 \text{ MeV}$. By taking $\alpha \approx 1$ the observer $\nu + \bar{\nu}$ energy per neutron is $\epsilon \approx 0.1 \Gamma_{nf} / (1+z) \text{ GeV}$, and the effective detection cross section per neutron is $\bar{\sigma}_{\nu\bar{\nu}} \sim 5 \times 10^{-40} \Gamma_{nf} (1+z)^{-1} \text{ cm}^2$. Multiplying by a burst rate within a Hubble distance of $\mathcal{R}_b \sim 10^3 \mathcal{R}_{b3}/\text{yr}$, for a 1 km^3 detector containing $N_t \sim 10^{39} N_{t39}$ target protons, the rate $R_{\nu\bar{\nu}} = (N_t/4\pi D_p^2) \mathcal{R}_b N_n \bar{\sigma}_{\nu\bar{\nu}}$ is

$$\begin{aligned} R_{\nu\bar{\nu}} &\sim 7 E_{53} N_{t39} \mathcal{R}_{b3} \left(\frac{2\xi}{1+\xi} \right) \left(\frac{\eta_\pi}{\eta} \right)^{4/3} \\ &\times h_{65}^2 \left(\frac{2 - \sqrt{2}}{1+z - \sqrt{1+z}} \right)^2 \text{ year}^{-1} \end{aligned} \quad (7)$$

events in the detector in coincidence with GRB electromagnetic flashes. The energies of the events are

$$\epsilon_{\nu_\mu \bar{\nu}_\mu} \sim 10 \text{ GeV}, \quad \epsilon_{\nu_e \bar{\nu}_e} \sim 5 \text{ GeV}, \quad (8)$$

which scale $\propto E_{53}^{1/4} t_{w1}^{-1/4} r_{o7}^{-1/4} (2/[1+\xi])^{1/4} (2/[1+z]) (\eta_\pi/\eta)^{1/3}$.

Subsequent to decoupling and n, p collisions, each neutron decay $n \rightarrow p + e^- + \bar{\nu}_e$ leads to an additional $\bar{\nu}_e$ of c.m. energy $\epsilon'_{\bar{\nu}_e, d} \sim 0.8 \text{ MeV}$, which when boosted in the observer frame by $\Gamma_{nf}/(1+z)$ is $\lesssim 120 \text{ MeV}$. The cross section is $\sigma_{\bar{\nu}_e} \sim 2 \times 10^{-40} \text{ cm}^2$ and the expected rate in a km^3 detector is less than one event per year.

IV. MeV γ rays.—The nonthermal MeV γ rays are thought to be produced in collisionless shocks [10], which occur at a radius $r_{sh} > r_\gamma > r_\pi$, after the bulk Lorentz factor has saturated to its asymptotic value. For an n, p outflow, shocks can occur in the original p , as well as in the n component after the latter has decayed, and this can influence the external shock light curves [11]. A separate and important consequence of neutron decay is that it should also affect the internal shock gamma-ray light curves. In the proton component, internal shocks occur at $r_{sh} \sim ct_v \Gamma_{pf}^2$, where t_v is the variability time

scale, and Γ_{pf} is the asymptotic proton Lorentz factor. From energy conservation, for $\eta > \eta_\pi$ this is $\Gamma_{pf} \sim \eta(1+\xi)[1 - (\xi/[1+\xi])](6/7)(\eta_\pi/\eta)^{4/3}$, and taking into account photon drag, one can show that an upper limit is $\Gamma_{pf, \max} \lesssim 8.3 \times 10^2 E_{53}^{1/4} t_{w1}^{-1/4} r_{o7}^{-1/4} (1+8\xi/7)^{1/4}$.

The γ rays start to arrive at an observer time $t \sim t_v \gtrsim 10^{-3} t_{v-3} \text{ s}$, lasting for a time t_w (where $10^{-3} \lesssim t_w \lesssim 10^3 \text{ s}$). For the n component, $r_{sh} \sim ct_{\min} \Gamma_{nf}^2$, with Γ_{nf} from Eq. (3) and $t_{\min} \sim \min[t_v, t'_n \Gamma_{nf}^{-1}]$, where $t'_n \sim 10^3 \text{ s}$ is the comoving frame neutron decay time. By taking $\xi \sim 1$ in the estimates below, for $20 \lesssim \eta \lesssim \eta_\pi \sim 400$ the neutrons decay and shock beyond the proton shock for any $t_v \lesssim 10^3 \eta^{-1}$, at observer times $t_n = [50\text{s}, 3\text{s}]$, while for $\eta \gtrsim \eta_\pi \sim 400$ the neutrons decay and shock beyond the proton shock for any $t_v \lesssim 3(\eta_\pi/\eta)^{1/3} \text{ s}$. The typical observed duration of the decay, including the blue shift due to the bulk motion towards the observer, is $t_n \sim 10^3/\Gamma_{nf}$, where $\Gamma_{nf} \approx \eta$ for $\eta < \eta_\pi$ and $\Gamma_{nf} = (3/4)\eta_\pi(\eta/\eta_\pi)^{-1/3}$ for $\eta \geq \eta_\pi$. Thus t_n decreases from approximately 50 to 3 s for $20 \lesssim \eta \lesssim \eta_\pi \sim 400$, and then slowly increases again as $t_n \sim 3(\eta/\eta_\pi)^{1/3}$ for $\eta \gtrsim \eta_\pi \sim 400$, with both η_π and t_n scaling $\propto [(1+\xi)/2]^{-1/4}$.

The number of neutron decays is $\propto 1 - \exp(-t/t_n)$, so the envelope of the neutron-related light curve is the mirror image of a ‘‘fred’’ (fast rise–exponential decay), i.e., an ‘‘anti-fred’’ (or generally, slow rise–fast decay). In general, photon emission starts at t_v from the proton-related component, which lasts a time t_w with an arbitrary shape envelope, modulated by spikes of minimum duration $t_v < t_w$, depending on the chaotic behavior of the central engine producing the outflow. The neutron-related component starts at a later time $t_n > t_v$, and has an anti-fred shaped envelope modulated by spikes of t_v and a total duration t_w . If $t_w > t_n$, the anti-fred component would be hard to distinguish because of the superposition of the ongoing p and n components. However, for short bursts with $t_w < t_n \sim 3 \text{ s}$, the p and n components are separated: first there is a pulse of duration t_w with a random envelope, followed after a time $\sim t_n$ by a pulse with an anti-fred envelope of duration t_n , and characteristic photon energy softer than the previous by $\epsilon_n/\epsilon_p \sim t_w/t_n$ (which if small could be below the BATSE band, but may be detectable with the Swift satellite [12]). The latter pulse is a signature for neutron decay in the burst.

V. Discussion.—For characteristic parameters, GRB outflows produce 5–10 GeV $\nu_\mu \bar{\nu}_\mu$ and $\nu_e \bar{\nu}_e$ from internal inelastic p, n collisions that create pions. The $\nu\bar{\nu}$ energy output $E_{\nu\bar{\nu}} \sim 5 \times 10^{51} E_{53} (2\xi/[1+\xi]) (2/[1+z]) (\eta_\pi/\eta)^{4/3} \text{ ergs}$, depends on the total energy E of the GRB and on the neutron fraction ξ as well as on the dimensionless entropy η . For a km^3 detector, approximately 5–10 neutrino events above 10 GeV are predicted per year, for a neutron/proton ratio $\xi = 1$. These events will be coincident with GRB electromagnetic flashes

in direction and in time (to an accuracy of ~ 10 s), which can enable their separation from the atmospheric neutrino background. Underground water detectors of the type being planned by BAIKAL [13], NESTOR [14], ANTARES [15], and the Antarctic detector ICECUBE [16] could potentially detect these relatively low-energy neutrino events if a sufficiently high density of phototubes were used. About 80% of these neutrinos are ν_μ and $\bar{\nu}_\mu$ (in approximately equal numbers) and the remainder are ν_e and $\bar{\nu}_e$. These 5–10 GeV $\nu\bar{\nu}$ are followed by ~ 120 MeV $\bar{\nu}_e$ from neutron decay, but the event rate from neutron-decay neutrinos is very low. The higher-energy neutrinos are produced for neutron/proton ratios $\xi > 0$ when the dimensionless entropy $\eta = L/Mc^2$ exceeds $\eta_\pi \approx 4 \times 10^2 L_{52}^{1/4} r_{07}^{-1/4} (2/[1 + \xi])^{1/4}$, and are accompanied by ~ 10 GeV photons which may be detectable in low redshift cases with GLAST [8]. For a typical GRB at redshift $z \sim 1$ the number fluences in 10 GeV neutrinos are $N(\bar{\nu}_e + \nu_e) \sim 0.5N(\bar{\nu}_\mu + \nu_\mu) \sim 10^{-4} \text{ cm}^{-2}$, and 1 order of magnitude less for GeV photons.

In all bursts where $\xi > 0$ the lower energy (~ 120 MeV) neutrinos are produced, and neutron decay occurs on an observer time scale $t_n \sim 3L_{52}^{-1/4} r_{07}^{1/4} [(1 + \xi)/2]^{1/4} (\eta/\eta_\pi)^{1/3}$ s. For outflows of duration t_w , these decays will be associated with MeV electromagnetic pulses of duration $\min[t_n, t_w]$, which are additional to the MeV pulses expected from shocks in the original proton component. For short bursts with $t_w \lesssim 3$ s, the proton electromagnetic pulse appears first and is separated from a subsequent neutron electromagnetic pulse, the latter having a slow rise–fast decay envelope and a softer spectrum, which may be detectable with the Swift satellite [12]. A systematic study of the time histories of GRB emission would be useful to search for evidence of delayed pulses that might be caused by neutron decay.

The detection of 5–10 GeV $\nu\bar{\nu}$ in coincidence with GRB photon flashes would not be easy, but would provide unique astrophysical information. Constraints on the neutron fraction could provide information about the progenitor stellar system giving rise to GRB. For instance, core collapse of massive stars would lead to an outflow from a Fe-rich core with $\xi \sim 2/3 - 1$, while neutron star mergers would imply $\xi \geq 1$. Photodissociation during collapse or merger, as well as n, p decoupling and inelastic collisions, would drive ξ toward unity, although this equalization process is likely to remain incomplete. For low $\eta \lesssim \eta_\pi$, inelastic collisions are not expected and the 5–10 GeV $\nu\bar{\nu}$ are absent, producing only the harder to detect ~ 100 MeV $\bar{\nu}_e$ from neutron decay. An initially non-baryonic outflow of, e.g., e^\pm and magnetic fields, would

acquire a baryonic load by entrainment from the progenitor environment, with $\xi \ll 1$ from massive stellar envelopes, but $\xi \geq 1$ for, e.g., compact mergers. Thus, lower values of ξ , leading to lower ratios of 5–10 GeV $\nu\bar{\nu}$ and a lower ratio of neutron decay MeV photons to total fluences, would be expected from massive progenitors rather than from compact mergers.

Partial support was received by J.N.B. from NSF PHY95-13835 and by P.M. from NASA NAG5-2857, the Guggenheim Foundation, and the Institute for Advanced Study. We acknowledge valuable conversations with G. Fishman, V. Fitch, V.I. Kocharovskiy, P. Kumar, R. Nemiroff, J. Norris, M. J. Rees, P. Vogel, and E. Waxman.

-
- [1] G. J. Fishman and C. A. Meegan, *Annu. Rev. Astron. Astrophys.* **33**, 415 (1995); J. van Paradijs, C. Kouveliotou, and R. Wijers, *Annu. Rev. Astron. Astrophys.* (to be published).
 - [2] P. Mészáros, *Prog. Theor. Phys.* (to be published) (astro-ph/9912546).
 - [3] E. V. Derishev, V. V. Kocharovskiy, and V. I. Kocharovskiy, *Astrophys. J.* **521**, 640 (1999).
 - [4] E. Waxman and J. N. Bahcall, *Phys. Rev. Lett.* **78**, 2292 (1997); E. Waxman and J. N. Bahcall, hep-ph/9909286; M. Vietri, *Phys. Rev. Lett.* **80**, 3690 (1998); J. Rachen and P. Mészáros, *Phys. Rev. D* **58**, 123005 (1998).
 - [5] B. Paczyński and G. Xu, *Astrophys. J.* **427**, 708 (1994).
 - [6] P. Kumar, *Astrophys. J.* **523**, L113 (1999).
 - [7] J. Catelli, B. Dingus, and P. Schneider, in *Gamma-Ray Bursts*, edited by C. Meegan *et al.*, AIP Conf. Proc. No. 42B (AIP, New York, 1998), p. 309.
 - [8] N. Gehrels and P. Michelson, *Astropart. Phys.* **11**, 277 (1999).
 - [9] T. K. Gaisser, *Cosmic Rays and Particle Physics* (Cambridge University Press, Cambridge, England, 1990); P. Vogel, *Phys. Rev. D* **29**, 1918 (1984).
 - [10] M. J. Rees and P. Mészáros, *Astrophys. J.* **430**, L93 (1994).
 - [11] E. V. Derishev, V. V. Kocharovskiy, and V. I. Kocharovskiy, *Astron. Astrophys.* **345**, L51 (1999).
 - [12] Swift homepage, <http://swift.gsfc.nasa.gov/>
 - [13] I. A. Beloplatikov *et al.*, *Astropart. Phys.* **7**, 263 (1997).
 - [14] L. Trascatti, in special issue on *Proceedings of the 5th International Workshop on Topics in Astroparticle and Underground Physics (IAUP97), Gran Sasso, Italy*, edited by A. Bottini *et al.*, *Nucl. Phys.* **B70**, 442 (1998).
 - [15] F. Feinstein, in special issue on *Proceedings of the 5th International Workshop on Topics in Astroparticle and Underground Physics (IAUP97), Gran Sasso, Italy* (Ref. [14]), p. 445.
 - [16] F. Halzen in *Proceedings of the 17th International Conference on Weak Interactions and Neutrinos, Cape Town, South Africa, 1999* (to be published) (astro-ph/9908138).